A&A 406, L1–L4 (2003)
DOI: 10.1051/0004-6361:20030810

Astronomy & Astrophysics

Two-dimensional simulations of the line-driven instability in hot-star winds

L. Dessart[1] and S. P. Owocki[2]

[1] Max-Planck Institute für Astrophysik, Karl-Schwarschild-Str. 1, 85740 Garching bei München, Germany
[2] Bartol Research Institute of the University of Delaware, Newark, DE 19716, USA
e-mail: owocki@bartol.udel.edu

Received 23 April 2003 / Accepted 26 May 2003

Abstract. We report initial results of two-dimensional simulations of the nonlinear evolution of the line-driven instability (LDI) in hot-star winds. The method is based on the Smooth Source Function (SSF) formalism for nonlocal evaluation of the radial line-force, implemented separately within each of a set of radiatively isolated azimuthal grid zones. The results show that radially compressed "shells" that develop initially from the LDI are systematically broken up by Rayleigh-Taylor or thin-shell instabilities as these structures are accelerated outward. Through radial feedback of backscattered radiation, this leads ultimately to a flow structure characterized by nearly complete lateral incoherence, with structure extending down to the lateral grid scale, which here corresponds to angle sizes of order a fifth of a degree. We briefly discuss the implications for interpreting various observational diagnostics of wind structure, but also emphasize the importance of future extensions to include lateral line-drag effects of diffuse radiation, which may set a minimum lateral scale for break-up of flow structure.

Key words. line: formation – radiative transfer – stars: atmospheres – stars: early type – stars: mass loss

1. Introduction

The driving of hot-star winds by line-scattering of the star's radiation is understood to be highly unstable to small-scale perturbations (Lucy & Solomon 1971; MacGregor et al. 1979; Owocki & Rybicki 1984, 1985). This "Line-Driven-Instability" (LDI) has long been supposed to be a root cause of the extensive small-scale wind structure that has been inferred from various kinds of observational diagnostics (e.g., soft X-ray emission; black troughs in saturated UV wind lines; nonthermal radio emission; emission line variability – see reviews by, e.g., Owocki 1994; Feldmeier & Owocki 1998; Dessart 2003). But a key limitation in developing quantitative tests of this supposition is that, owing to the computational expense of evaluating nonlocal integrals needed for calculating the line-force, time-dependent dynamical simulations of the resulting nonlinear flow structure (Owocki et al. 1987; Feldmeier et al. 1997; Owocki & Puls 1999; Runacres & Owocki 2002) have so far generally been limited to one dimension (1D) (see, however, Owocki 1998 and Gomez & Williams 2003). These 1D simulations show development of extensive radial variations in both density and radial velocity, but are inherently incapable of determining the development of any corresponding variations in the *lateral* direction.

In this Letter we report on initial results of two-dimensional (2D) simulations that, for tractibility, employ a restricted approach we dub "2D-H+1D-R" (2D Hydrodynamics + 1D Radiation). This follows both the radial and lateral evolution of velocity and density, but assumes the line-force is strictly *radial*, computed by nonlocal radial-coordinate integrations that are isolated along a single ray within each azimuthal cone (see Sect. 2). (Such a scheme lends itself naturally to parallelization for computer clusters.) The results (Sect. 3) show that the initial "shells" of radial compression that arise from the LDI tend eventually to be broken up by Rayleigh-Taylor or thin-shell (Vishniac 1994) instabilities at the smallest azimuthal scale, which here is set to correspond roughly to the few tenths of a degree scale at which the "line-drag" effect (Lucy 1984) of a lateral diffuse radiation force (Rybicki et al. 1990) would be expected to damp any wind structure. We conclude by briefly discussing (Sect. 4) the potential implications for interpreting the various diagnostics of wind structure.

Send offprint requests to: L. Dessart,
e-mail: luc@mpa-garching.mpg.de

2. Method

We carry out our simulations using the public domain hydrodynamics code ZEUS (Stone & Norman 1992), operated in a spherical coordinate system with the colatitude fixed at the equator ($\theta = 90°$), but allowing for variations in both radius r and azimuth ϕ, resolved through a spatial grid of n_r by n_ϕ mesh points. The specific results detailed here are based on a standard configuration of $n_r = 1000$ radial zones. These start from a lower boundary at the stellar surface radius $r_0 = R_*$ with an initial step size of $\mathrm{d}r_0 = 0.002R_*$, which then increases

by 0.813% per zone for 200 zones to equal $\mathrm{d}r_{200} = 0.01R_*$ at $r_{200} \approx 2R_*$. The remaining 800 zones then use this as a constant step size out to an outer boundary radius $r_{1000} = 10R_*$.

For the lateral mesh, it seems most appropriate to choose a step size in azimuthal angle that gives a grid aspect ratio near unity in the wind acceleration region $r = 1{-}2\,R_*$, where unstable structures are first manifest. Since in this region $\mathrm{d}r/r \approx 0.002{-}0.005\,\mathrm{rad} \approx 0.1{-}0.3^\circ$, we choose a fixed azimuthal grid size $\mathrm{d}\phi = 0.2^\circ$. To allow this high lateral resolution with a moderate number of $n_\phi = 60$ azimuthal zones, we restrict the lateral mesh to a narrow "wedge" with azimuthal range $\Delta\phi = n_\phi \times \mathrm{d}\phi = 12^\circ$, over which we then apply periodic boundary conditions, implemented by setting all hydrodynamic variables (i.e., density ρ, radial velocity v_r, and azimuthal velocity v_ϕ) to equal values between the left and right interfaces (e.g. for density, $\rho(r_i, \phi_0) = \rho(r_i, \phi_{n_\phi})$).

The radial boundary conditions and stellar parameters (characteristic of a typical O-supergiant like ζ Puppis) are as given in the previous 1D simulations of Dessart & Owocki (2002a). We assume an isothermal equation of state with the wind temperature set to the stellar effective temperature.

The (strictly radial) line-force is computed using the Smooth Source Function (SSF) formalism (Owocki 1991; Owocki & Puls 1996, 1999), implemented within our 2D-H+1D-R approach by a radial-mesh integration of the line-ensemble, frequency-averaged optical depth, evaluated separately in each of the n_ϕ azimuthal zones. The line-ensemble parameters and the boundary value frequency profiles for the upward and downward streaming optical depth at the inner and outer radii are as given by Dessart & Owocki (2002a). This SSF formalism accounts for both the direct force component that gives rise to the LDI, as well as the diffuse component that leads to a "line-drag" effect (Lucy 1984). The latter reduces, but does not eliminate, the net growth rate of the instability to radial velocity perturbations on scales near and below the radial Sobolev length $l_1 \equiv v_\mathrm{th}/(\mathrm{d}v_\mathrm{r}/\mathrm{d}r)$ (over which the radial flow accelerates by an ion thermal speed v_th) (Owocki & Rybicki 1985).

But the avoidance here of the *lateral* integration needed to compute an azimuthal component of the diffuse line-force means that we are ignoring a potentially strong net lateral line-drag that should strongly damp azimuthal velocity perturbations on scales below the lateral Sobolev length $l_0 \equiv rv_\mathrm{th}/v_\mathrm{r}$ (Rybicki et al. 1990). Presuming that this inhibits development of lateral instability at such scales, then any lateral breakup would be limited to a minimum lateral angular scale of $\Delta\phi_\mathrm{min} \approx l_0/r = v_\mathrm{th}/v_\mathrm{r} \approx 0.01\,\mathrm{rad} \approx 0.5^\circ$. This provides further justification for our choice here of a comparable value for the azimuthal grid size, $\mathrm{d}\phi = 0.2^\circ$, but clearly future work should readdress this issue through explicit incorporation of the lateral line-force and the associated line-drag effect.

The initial condition is set from the standard CAK (Castor et al. 1975) steady-state model, which applies the Sobolev (1960) approximation to compute the line-force in terms of the *local* velocity gradient and density, and thus does not account for instabilities on scales near and below the radial Sobolev length. The use of the SSF line-force in the subsequent time evolution allows one to follow the nonlinear development of these small-scale instabilities. For this we do not need to introduce any explicit perturbations into the flow or photospheric wind base. Indeed, as in previous 1D simulations (e.g., Owocki & Puls 1999; Dessart & Owocki 2002a,b), once structure develops, e.g. from the initial adjustments to the CAK starting condition, radiative backscattering from the outer to inner wind seeds small-amplitude base fluctuations that are then strongly amplified by the LDI as the flow is accelerated outward. This thus perpetuates an entirely *intrinsic* formation of wind structure.

3. Results

Results for the time evolution of 2D flow structure are illustrated in Fig. 1, which shows polar coordinate greyscale plots for the relative deviations from the CAK steady solutions for (a) density, (b) radial velocity, and (c) azimuthal velocity. These figures employ a rather novel "clock format", in which the state snapshot in each azimuthal wedge of $\Delta\phi = 12^\circ$ is repeated as a time sequence, starting from the 12 o'clock position and proceeding clockwise at fixed time intervals of 4000 s.

Starting from the initial smooth CAK state, the LDI is first manifest as strong radial velocity variations and associated density compressions that initially extend nearly coherently across the full azimuthal range of the computational wedge. But as these initial "shell" structures are accelerated outward, they become progressively disrupted by Rayleigh-Taylor or thin-shell (Vishniac 1994) instabilities that operate in azimuth down to the grid scale $\mathrm{d}\phi = 0.2^\circ$. Within the SSF formalism applied through separate radial integrations in each azimuthal zone, the lateral phase variations that arise in the outer wind of this initial structure lead – through the backscattering component of the diffuse radiative force – to corresponding lateral phase variations in small-amplitude fluctuations induced near the wind base. As these now laterally varying fluctuations are amplified within the separate radial propagation in each azimuthal zone, the outer wind structure becomes evermore broken up. By the time $t = 4000 \times 360/12 = 120\,000$ s of the final state shown here (just before 12 o'clock in Figs. 1a–c), the wind is thus characterized by a nearly complete lateral incoherence down to angular scales approaching that of the azimuthal grid.

Figure 2 shows line plots of the radial variation of various azimuthally and temporally averaged measures of the flow properties. Since we ignore any lateral component of the line-force, the variations in azimuthal velocity arise completely from lateral variations in gas pressure, and so have a typical rms amplitude $\Delta v_{\phi,\mathrm{rms}} \approx 10{-}15\ \mathrm{km\,s^{-1}}$ comparable to the sound speed $a = 24\ \mathrm{km\,s^{-1}}$. The structure in density and radial velocity are a direct outcome of the LDI. The lateral "filling in" of radial rarefactions leads here to a significantly lower density "clumping factor" $f_\mathrm{cl} \equiv \langle\rho^2\rangle/\langle\rho\rangle^2 \approx 3{-}5$ (with angle brackets representing temporal and/or azimuthal averaging) than is typically found in analagous 1D LDI simulations, which have $f_\mathrm{cl} \gtrsim 10$ (Runacres & Owocki 2002). On the other hand, the possibility for lateral velocity shear now allows high-speed rarefactions to flow past slower, localized density enhancements, instead of being abruptly truncated as they are in purely radial models. As a result, the radial velocity

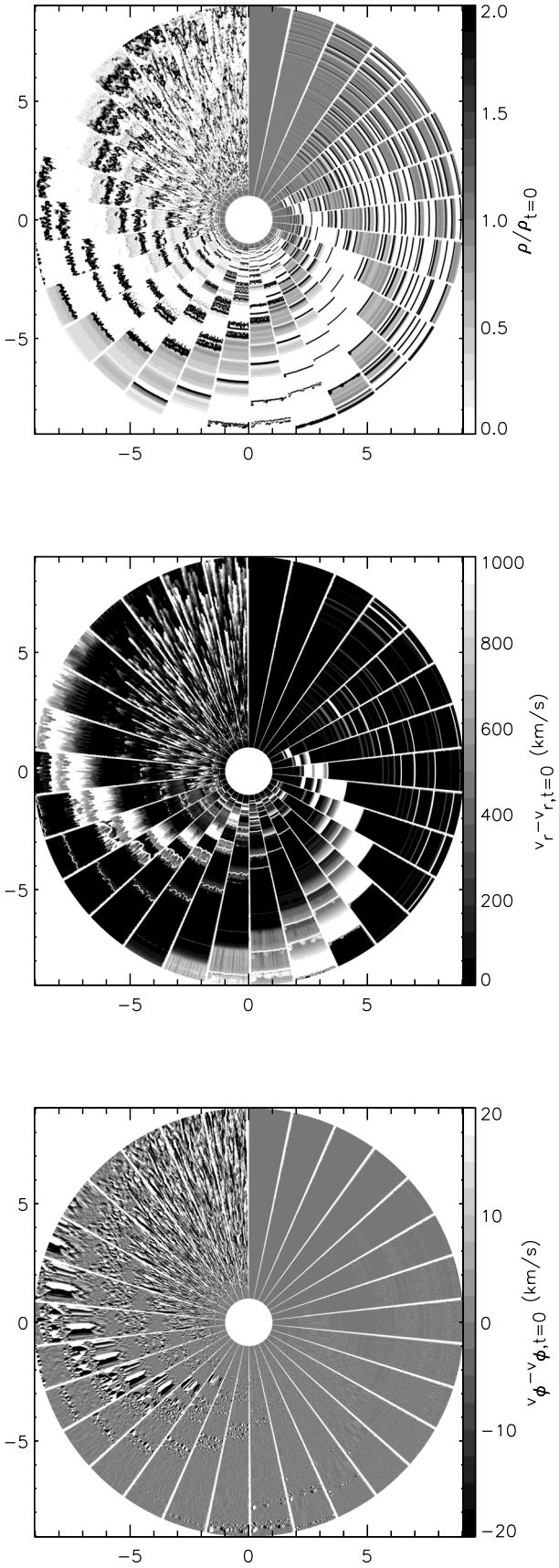

Fig. 1. Grayscale representation for the deviations of **a)** density, **b)** radial velocity, and **c)** azimuthal velocity, rendered as a time sequence of the 2D wedges of $\Delta\phi = 12^\circ$ stacked clockwise from the vertical in intervals of 4000 s.

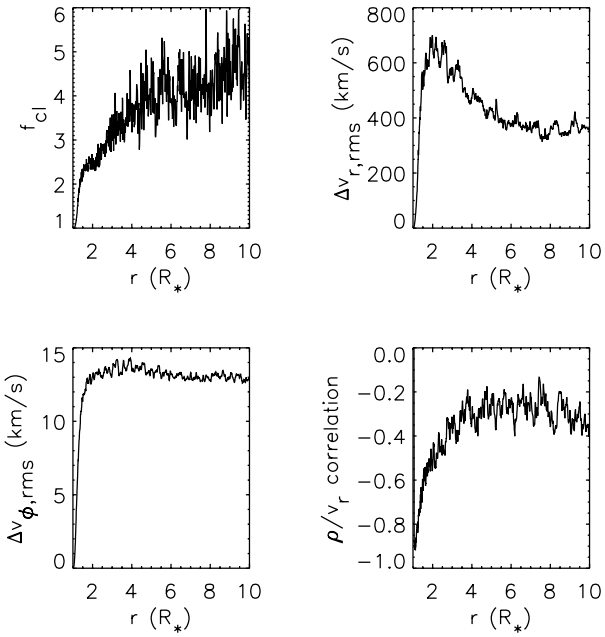

Fig. 2. Radial variation of temporal and azimuthal averages that characterize the nature of flow structure. **a)** clumping factor $f_{\rm cl}$; **b)** radial and **c)** azimuthal velocity dispersion; and **d)** velocity-density correlation coefficient (Runacres & Owocki 2002).

dispersion in these 2D simulations, $\Delta v_{\rm r,rms} \approx 400{-}700$ km s^{-1}, is actually somewhat *higher* that in corresponding 1D models, $\Delta v_{\rm r,rms} \approx 200{-}300$ km s^{-1}.

Instead of azimuthally extended shells, the overall effect of this strong lateral shear of the radial velocity is to impart a "radial streaking" character to the flow structure. In other simulation runs done at various resolutions, we quite generally find that the smallest lateral structure extends down to the azimuthal grid size, although the time required for full development to this state increases with decreasing resolution. Further results of this extended resolution study will be given in a follow-on journal paper.

4. Discussion

These results have some potentially important implications for interpreting the various kinds of observational diagnostics for wind structure:

- The reduced density clumping implies a smaller correction to the estimated wind mass loss rates from recombination or other two-body processes, for which the true value is reduced in proportion to $1/\sqrt{f_{\rm cl}}$. The lower clumping value here seems more compatible with those inferred for Wolf-Rayet winds by Hillier & Miller (1998), based on comparison of linear-density strength of electron scattering wings vs. the density-square strength of the overall line emission.
- The increased radial velocity dispersion may help explain the observed soft X-ray emission from hot-stars, which is generally higher than can be readily produced by 1D instability simulations (Feldmeier et al. 1997).

– The azimuthal scale of structure found here is substantially smaller than the optimal ca. 3° "patch size" inferred for reproducing the amplitude and wavelet spectrum of emission line variability in Wolf-Rayet winds (Dessart & Owocki 2002a,b). The small scales also mean that the individual dense structures tend to accelerate along with the mean wind, and so would not readily reproduce the slow apparent accelerations characteristic of observed emission line variations (Lepine 1995; Lepine & Moffat 1999).

Overall the picture presented by these simulations differs markedly from previous ideas of radially compressed shell structures. The general finding of disruption by lateral instabilities seems likely to be a quite robust result. But establishing the exact limiting angular scale will require further studies that include the lateral transfer of diffuse radiation. This could limit the smallest lateral scale in two ways. The first is through lateral averaging of variation in the diffuse, backscattered radiation that leads to structure self-excitation at the wind base. The second is through the lateral line-drag effect that could suppress unstable growth at the smallest lateral scales in the outer wind. Developing methods for tractable computation of the lateral component of the diffuse line-force should thus be a principal focus of future studies of the multidimensional nature of wind structure generated by the line-driven instability.

Acknowledgements. SPO acknowledges support of NASA grants NAG5-11886 and NAG5-11095, and NSF grant AST-0097983, awarded to the University of Delaware, and an UK-PPARC Visitor Fellowship. He thanks J. Brown at University of Glasgow and A. Willis at University College London for their hopitality during his sabbatical visit to these institutions.

References

Castor, J. I., Abbott, D. C., & Klein, R. I. 1975, ApJ, 195, 157 (CAK)
Dessart, L., & Owocki, S. P. 2002a, A&A, 383, 1113
Dessart, L., & Owocki, S. P. 2002b, A&A, 393, 991
Dessart, L. 2003, in Massive Stars: Formation, Evolution, Internal Structure and Environnement, ed. M. Heydari-Malayeri, & J.-P. Zahn
Feldmeier, A., & Owocki, S. 1998, Ap&SS, 260, 113
Feldmeier, A., Puls, J., & Pauldrach, A. 1997, A&A, 322, 878
Gomez, E., & Williams, R. 2003, in Stellar Rotation, IAU Symp., 215, ed. A. Maeder, & P. Eennens
Hillier, D. J., & Miller, D. 1998, ApJ, 496, 407
Lépine, S. 1995, Ph.D. Thesis, Université de Montréal
Lépine, S., & Moffat, A. F. J. 1999, ApJ, 514, 909 (LM)
Lucy, L. B., & Solomon, P. M. 1970, ApJ, 159, 879
Lucy, L. B. 1984, ApJ, 284, 351
MacGregor, K. B., Hartmann, L., & Raymond, J. ApJ, 231, 514
Owocki, S. P. 1991, in Stellar Atmospheres: Beyond Classical Models, 235
Owocki, S. P. 1994, Astrophys. Sp. Sci., 221, 3
Owocki, S. P. 1999, in Variable and Non-spherical Stellar Winds in Luminous Hot Stars, 294
Owocki, S. P., Castor, J. I., & Rybicki, G. B. 1988, ApJ, 335, 914
Owocki, S. P., & Rybicki, G. B. 1984, ApJ, 284, 337
Owocki, S. P., & Rybicki, G. B. 1985, ApJ, 299, 265
Owocki, S. P., & Puls, J. 1999, ApJ, 510, 355
Rybicki, G. B., Owocki, S. P., & Castor, J. I. 1990, ApJ, 349, 274
Robert, C. 1992, Ph.D. Thesis, Université de Montréal
Sobolev, V. V. 1960, Moving Envelopes of Stars (Cambridge: Harvard University Press)
Stone, J. M., & Norman, M. L. 1992, ApJS, 80, 753
Vishniac, E. T. 1994, ApJ, 428, 186